ISSN 1023-1935, Russian Journal of Electrochemistry, 2010, Vol. 46, No. 5, pp. 501–511. © Pleiades Publishing, Ltd., 2010.
Original Russian Text © Yu.G. Chirkov, V.I. Rostokin, 2010, published in Elektrokhimiya, 2010, Vol. 46, No. 5, pp. 532–543.

Cathodic Active Layer in a Polymer Electrolyte Fuel Cell: Model of Combined Grains, Calculation of Overall Characteristics

Yu. G. Chirkov[z, a] **and V. I. Rostokin**[b]

[a] *Frumkin Institute of Physical Chemistry and Electrochemistry, Russian Academy of Sciences Leninskii pr. 31, Moscow, 119991 Russia*

[b] *Moscow Institute of Engineering Physics, Kashirskoe sh. 31, Moscow, 115409 Russia*

Received March 16, 2009

Abstract—A new type of the cathodic active layer structure for a polymer electrolyte fuel cell is proposed. This structure is based on combined grains and gas pores. Combined grains represent nonporous agglomerates of carbon black particles (catalyst carrier) and Nafion molecules. This type of cathodes has the following advantages: (1) in combined grains, complete utilization of the catalyst occurs, (2) limitations on the oxygen delivery into the active layer are almost totally lifted, and (3) the danger that pores will be flooded with evolved moisture is actually released. The overall characteristics of cathodes with combined grains are calculated. The advantages of such oxygen or air cathodes are demonstrated, namely, not only their enhanced power density but also the lower index of platinum consumption, i.e., the platinum amount per kW of electric energy produced in the membrane-electrode block, as compared with conventional cathodes.

Key words: fuel cell with Nafion and platinum, oxygen and air cathodes, computer simulation of the current generation process in an active layer, combined grains, calculation of the ionic conductivity of a combined grain, calculations of overall characteristics of a cathode with combined grains

DOI: 10.1134/S1023193510050034

INTRODUCTION

Low-temperature hydrogen-oxygen and hydrogen-air fuel cells continue to be among the major candidates for electrochemical power sources for autonomous space and earth units. Their efficiency in the conversion of chemical energy to electricity, i.e., such parameters as the power per weight unit (W/kg) and the power density (W/cm^2), are observed to increase. The first generation of fuel cells that employed hydrophilic biporous electrode with a barrier layer and operated at a pressure gradient made it possible to generate small overall currents of the order of magnitude of tenth fractions of A/cm^2. The second generation of fuel cells with hydrophobized porous electrodes demonstrated overall characteristics of several A/cm^2. The third generation of fuel cells with polymer electrolyte (usually Nafion) allowed very high currents of several tens of A/cm^2 to be generated.

However, commercialization of fuel cells depends not only on high overall currents and power densities but also on the catalyst consumption in cells. The point is that the main electrocatalyst employed in the most problematic part of a fuel cell, namely, in the cathodic active layer where oxygen is reduced in an acidic medium, is still platinum. However, its resources are extremely limited. At the same time, numerous attempts to find a substitute for platinum have not yet succeeded.

Thus, there is an urging demand for minimizing in every possible way the platinum consumption in fuel cells with polymer electrolytes. It is necessary that polymer electrolytes fuel cells exhibited not only the power density of an order of magnitude of several W/cm^2 but also the lowest possible index of platinum consumption (its amount per kW of electric energy generated in the membrane-electrode block (MEB).

For the most popular system, i.e., the hydrogen-air fuel cell with polymer electrolyte, a considerable but yet insufficient success has been achieved. For a MEB loaded with 0.6–0.8 mg/cm^2 of platinum at voltage of 0.6 V (which corresponds to 58% efficiency at 80°C and atmospheric pressure), the power density was raised to 0.7 W/cm^2 [1]. This corresponds to the specific consumption of platinum in the range of 0.85–1.1 g/kW.

These values point to considerable progress as compared with even the state-of-the-art with MEB in the recent 90s of the past century. At the same time, according to the authors of [2], for the hydrogen-air fuel cells with Nafion and platinum to attract attention in car manufacturers, the platinum consumption should be reduced 5-fold.

[z] Corresponding author: olga.nedelina@gmail.com (Yu.G. Chirkov).

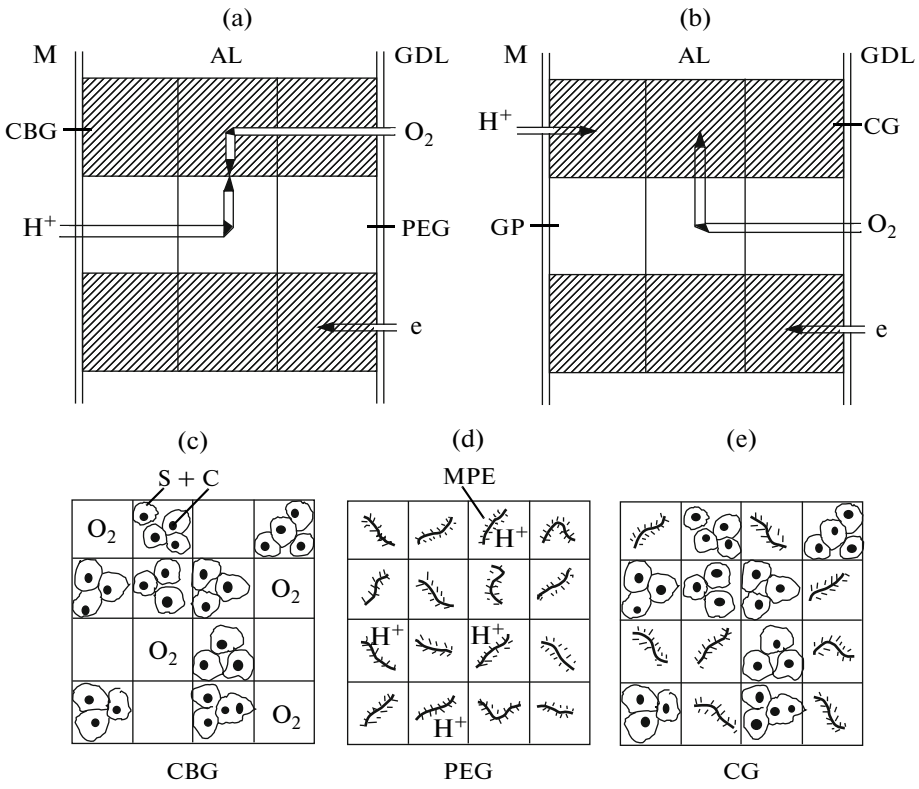

Fig. 1. Illustration of channels for the delivery of electrons (e), protons (H^+) and oxygen molecules (O_2) in the active layer of a cathode with polymer electrolyte in the framework of the "model of isomeric grains": (a) conventional active layer structure, (b) cathode with combined grains, (c) conditional presentation of the structure of catalyst carrier grains, (d) conditional presentation of polymer electrolyte grains, (e) conditional presentation of combined grains. M is the Nafion membrane in a fuel cell, AL is the active layer, GDL is the gas-diffusion layer, CBG is the carrier grain (carbon black) with platinum catalyst, PEG is the polymer electrolyte grain, CG is the combined grain, GP is the gas pore, S is the carbon black (soot) particles, C is the catalyst (platinum) particle, MPE is the polymer electrolyte molecule.

The goal of this study is to outline a way to substantially reduce the platinum consumption in the cathode active layer without any considerable loss in the fuel cell power density.

COMBINED GRAIN

A large number of studies were devoted to the mechanism of current generation in cathodes of fuel cells with Nafion and platinum [3–10]; however, many unsolved problems still remain. A simple "model of isomeric grains" was proposed [11] which proved to be convenient in carrying out computer simulations and estimating the overall characteristics of a cathode with Nafion. The grains represent isomeric agglomerates of the carrier of platinum (carbon black) and agglomerates of Nafion molecules. The "model of isomeric grains" made in possible [12] to explain why cathodes with Nafion demonstrated the power characteristics (power density above 1 W/cm^2) so high compared with hydrophobized cathodes. However, first of all it should be mentioned that even this perfect system of electrochemical current generation has also substantial drawbacks.

Let us consider Fig. 1a that illustrates channels (conditionally shown percolation clusters of the corresponding grain types) for the delivery of electrons (e), protons (H^+), and oxygen molecules (O_2) in an active layer of a cathode with Nafion. Here (and also in Fig. 1b), M is the membrane (of Nafion), AL is the active layer, GDL is the gas-diffusion layer, CBG are carrier grains (carbon black, Fig. 1c) with the platinum catalyst, PEG are polymer electrolyte grains (Nafion, Fig. 1d).

The mechanism of current generation in the active layer of a cathode with Nafion and platinum was discussed in detail in [13]. There, it was assumed that each grain (CBG and PEG, "model of isomeric grains") represents a cube with the edge L. A porous carrier grain is partly filled with carbon black particles (S, Fig. 1c) covered with catalyst fine crystals (C, Fig. 1c). Furthermore, it was assumed that carbon black agglomerates involved in CBG in Fig. 1c are all identical and also shaped as cubes with the edge d. And all of them together with separating voids (the latter

can be obviously represented as divided into identical "cubes" with the edge d) are arranged into a cubic network of nodes (according to the percolation theory [14–16]).

As was shown in [13], the optimal active layer structure is achieved when the volume concentrations of polymer electrolyte grains (agglomerates of Nafion molecules, Fig. 1d) g_e and carrier grains (porous agglomerates of carbon black, Fig. 1c) g_s are equal to one another $g_e = g_s = 0.5$. Thus, the proton delivery channel represents a percolation cluster of polymer electrolyte grains (illustrated in Fig. 1a), while the channel for the delivery of electrons and oxygen represents a percolation cluster of porous carrier grains (Fig. 1a). Moreover, the diffusion of gas through the fine pores in carrier grains proceeds in the Knudsen mode.

Figures 1a and 1c clearly demonstrate the main drawbacks of the current generation in the active layer of an electrode with Nafion. First, here, the current is generated mainly at the interface of the ionic and electronic clusters (vertical arrows in Fig. 1a), i.e., at the contact of carrier grains with Nafion grains. This is why a part of catalyst in a carrier grain (in its central part, Fig. 1c) turns out to be excluded from the current-generation process. Second, the effective coefficient of Knudsen diffusion of gas in the carrier grains is very small. According to calculations, with the fulfilled condition $g_e = g_s = 0.5$, the effective diffusion coefficient of oxygen in the active layer of a cathode with polymer electrolyte $D^* = 4.5 \times 10^{-4}$ cm^2/s. This leads to severe internal diffusion limitations. Third, such a gas-delivery channel turns out to be very vulnerable. Water formed at the current generation quickly fills the fine Knudsen pores, the oxygen delivery into the active layer bulk stops, and the overall characteristics of the cathode worsen.

These negative phenomena can be avoided by the changeover from the active layer structure shown in Fig. 1a that have already became traditional to a structure shown in Fig. 1b. We introduce a notion of "combined grain" (CG). The latter is based on a carrier grain (Fig. 1c) with voids completely filled with Nafion molecules. Figure 1e illustrates a combined grain. A comparison of Fig. 1c with Fig. 1e shows that whereas a conventional grain provides the delivery of electrons and oxygen molecules into the active layer, a combined grain being a part of a percolation cluster is capable of supplying electrons and protons. On the same time, the gas can be delivered into the active layer with combined grains through the gas pores-voids (GP, Fig. 1b) in the same manner as, for example, into the active layer of hydrophobized cathodes.

The transition to cathodes with combined grains makes it possible to eliminate many drawbacks intrinsic of the active layer version shown in Fig. 1a. First, a combined layer provides complete contact between platinum microparticles deposited on the carrier (carbon black) surface and the proton supplier, i.e., Nafion molecules. Hence, now all platinum in the carrier bulk takes part in the current generation and the degree of catalyst utilization $\eta = 100\%$. Second, in a cathode with combined grains, oxygen instead of being delivered into the active layer by fine Knudsen pores is now supplied via coarse (with diameter of several hundred nm and more) gas pores by the usual molecular diffusion mechanism. The effective diffusion coefficient characterizing a gas cluster (Fig. 1b) is now high, about $D^* = 10^{-1}$ cm^2/s. Hence, the internal diffusion limitations in an active layer with combined grains become small and can be neglected in the first approximation. And finally, third, in the cathode active layer with combined grains, there is no danger that fine gas pores get flooded with evolved moisture. Formed water can be easier removed from coarse pores by being drained into pores of the gas-diffusion layer.

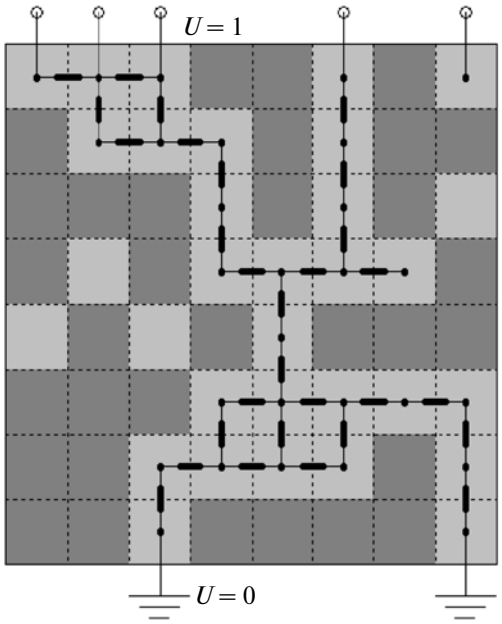

Fig. 2. A two-dimensional analogue of the network of nodes that models the proton conductivity through Nafion in a combined grain (carbon-black cells are shown dark grey, Nafion cells are light grey). Segments connecting the centers of those Nafion cells that can conduct protons model the conductivity units.

CALCULATION OF IONIC CONDUCTIVITY OF A COMBINED GRAIN

The aim of this section is to calculate the overall characteristics of a cathode with the active layer involving combined grains. For this purpose, it is necessary to calculate the specific ionic conductivity of a

combined grain and the specific ionic conductivity of the active layer with combined grains.

A polymeric electrolyte grain (Fig. 1d) has the ionic conductivity much higher than that of a combined grain (Fig. 1e), because Nafion fills the combined grain only partly and by channels of complicated geometry. When calculating the ionic conductivity of a combined grain (from hereon, we assume that in this grain, the volume fractions filled randomly with carbon black and Nafion are equal, Fig. 2), we used the model of regular geometrical "network of nodes" according to the notations of the percolation theory [14–16].

According to Fig. 2, the volume of a combined grain shaped as a cube was divided into equal "elementary" cells-microcubes of carbon black (agglomerates of carbon black particles, Fig. 1e) and Nafion cells (agglomerates of Nafion molecules). Each cell with proton-conducting Nafion is represented as an equivalent electric element of six units that have a common node corresponding to the Nafion cell center. Obviously, it is assumed that the Nafion conductivity is equal in the vertical and horizontal directions. The conductivity of each of these combined grains connecting the neighboring Nafion cells is assumed to be equal to k (ionic conductivity of Nafion). As a result, a network with the random distribution of conducting units and insulators (carbon black particles) that have zero conductivity is realized. It also deserves mention that not every Nafion cell can conduct current. Only units involved in a percolation cluster (Fig. 2) can contribute to conductivity. Such units should obviously be connected with the opposite sides of the combined grain under consideration.

The determination of ionic conductivity of a three-dimensional network of conducting and nonconducting cells was carried out using computer-assistant numerical simulations based on the Monte-Carlo method [17, 18]. In essence, this method is as follows. Network nodes are numbered with whole numbers (Fig. 2), Each unit connecting the ith and the kth nodes is characterized by the conductivity $g_{i,k}$. Then, according to Ohm's law, the current in this unit

$$j_{ik} = -g_{ik}(U_i - U_k). \quad (1)$$

For local currents, there is Kirchhoff's equation (the sum of currents converging in each node is zero), i.e.,

$$\Sigma g_{ik}(U_i - U_k) = 0, \quad (2)$$

where summation is carried out over all neighboring nodes that are connected with the ith node through the conducting units. From Kirchhoff's equation, it follows that if the currents are nonsteady-state, the potentials of the neighboring nodes are related by a relationship

$$U_i = \Sigma(g_{ik}U_k)/\Sigma g_{ik}. \quad (3)$$

In our case, the conductivities of all units connecting the Nafion centers are equal to $g_{ik} = \kappa$. Hence, the last equation is reduced to the equality

$$U_i = \Sigma U_k/m, \quad (4)$$

where m is the number of neighboring nodes through which a given node is connected with the conducting unit.

The potential U in each node of the upper ("frontal", nodes 1–3 and 4 in Fig. 2) layer of units is assumed to be equal to 1, whereas in the nodes of the opposite layer ("back", nodes 26 and 27 in Fig. 2), the potential is equal to zero (these potentials remain unchanged in the course of numerical iterations). The potentials of internal nodes U_i are set in the arbitrary manner in the range of 0–1 in the beginning of calculations.

For each node located in the center of the Nafion cell, the numerical solution of Kirchhoff's equation in the form (4) is sought, namely, the node potential is found as the averaged potential of all surrounding neighboring nodes in the Nafion cells. The nodes are considered layer-by-layer in the direction from the frontal boundary of the network to its back boundary. After the first run over all cells, a considerable redistribution of the potential is possible. However, at next iterations, the potential distribution ultimately acquires its stationary form. The iterations are finished when the difference of currents at the frontal and back boundaries of the studied sample (Fig. 2) becomes negligibly small.

The current at the frontal boundary is calculated as the sum of currents from a node with the potential $U = 1$ to the nearest Nafion node in the next layer

$$I_\Phi = \Sigma\kappa(1 - U_n), \quad (5)$$

where summation is carried out over all Nafion nodes of the mentioned layer. Analogously, the current through the back surface of the network is determined by the following equality:

$$I_T = \Sigma\kappa U_m, \quad (6)$$

where summation is carried out over all nodes that have access to the back boundary with the potential $U = 0$.

The effective conductivity of each particular configuration of the model network is determined as the ratio of the current in the system to the potential difference on the external boundaries, namely, $\kappa^{**} = I/\Delta U = I$, because we assume $\Delta U = 1$. The average statistical values of effective conductivity was estimated by averaging the value κ^{**} over $n = 1000$ different random distributions of carbon black and Nafion cubes in a combined grain, assuming 50% volume concentration of Nafion in the combined grain.

Figure 3 and Table 1 show the results of calculations of the dependence of the reduced ionic conduc-

tivity of a combined grain κ^{**} on its reduced dimensions $N = L/d$, i.e, on the number of cells of carbon black and Nafion located randomly along the combined grain edge. Obviously, for $N = 1$ (the combined grain is a microcube completely filled with Nafion molecules), $\kappa^{**} = 1$.

A combined grain in turn enters into the composition of a percolation ionic cluster (Fig. 1b); therefore, the specific ionic conductivity of the active layer with combined grains κ^{***} should be found from the following expression:

$$\kappa^{***} = \kappa\kappa^{**}\kappa^{*}, \quad (7)$$

where we assume that $\kappa = 0.1\ \Omega^{-1}\ cm^{-1}$ is the conductivity of Nafion with the optimal moisture content. In Eq. (7), κ^{**} is the reduced ionic conductivity of a combined grain (thus, the product $\kappa\kappa^{**}$ represents the ionic conductivity of a combined grain), κ^{*} is the reduced ionic conductivity of combined grains involved in a percolation ionic cluster. The latter value was determined in [11]. Its dependence on the volume concentration of combined grains g_s is shown in Table 2.

In Table 2, the range of possible concentrations of combined grains should be limited by the interval $0.35 < g_s < 0.65$, because a ionic percolation cluster is formed only on reaching a critical concentration g_s^* equal to [19]

$$g_s^* = [(1 + 2^{1/2})^{1/3} + (1 - 2^{1/2})^{1/3}]/2 = 0.298, \quad (8)$$

whereas at $g_s \geq 0.7$, in the active layer with combined grains, the formation of a gas percolation is obviously impossible.

According to the studies of the microstructure of the active layer on electrodes with polymer electrolyte [20], the size of bunches of carrier particles (carbon black, Fig. 1c) ≈20–40 nm, the size of agglomerates of carbon black particles (carrier grains) ≈200–300 nm. The pores between bunches of carbon black particles are in the same range of sizes, ≈20–40 nm, and filled with agglomerates of polymer electrolyte molecules either partly or completely. We assume that in combined grains, the size of carbon black cubes and Nafion cubes (Fig. 2) $d = 30$ nm, and the combined grain size $L = Nd$, where N is an even natural number, e.g., 2, 4, 6, etc.

In estimating the overall characteristics of cathodes with combined grains, it is reasonable to assume that the volume concentration of combined grains is maximally large $g_s = 0.65$. In this case, according to Table 2, the reduced ionic conductivity of combined grains involved in a percolation cluster reaches its maximum value $\kappa^{*} = 0.304$; hence, the overall current obtained on a cathode with combined grains is also maximum. In this case, the active layer conductivity κ^{***} is determined by the reduced size of a combined grain N.

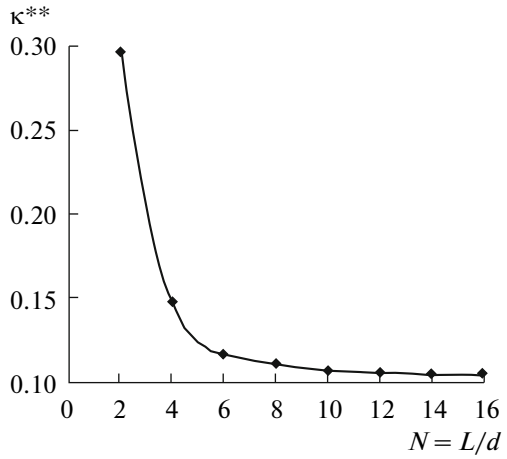

Fig. 3. Dependence of the reduced ionic conductivity of a combined grain κ^{**} on its reduced size N.

Let us use the data in Table 2. According to Eq. (7), we obtain that the maximum of ionic conductivity of an active layer with combined grains κ^{***} will be reached at $N = 2$ (the length of edges of a combined grain $L = 60$ nm), then $\kappa^{***} = 9.06 \times 10^{-3}\ \Omega^{-1}\ cm^{-1}$. With the increase in N, the conductivity κ^{***} first quickly decreases (Fig. 3) to reach a value $\kappa^{***} = 3.37 \times 10^{-3}\ \Omega^{-1}\ cm^{-1}$ at $N = 8$ (when the combined grain edge $L = 240$ nm) an then attains a virtually constant value $\kappa_{\infty}^{***} = 0.1 \times 0.105 \times 0.304 = 3.04 \times 10^{-3}\ \Omega^{-1}\ cm^{-1}$.

CHOICE OF THE CRITERION OF ESTIMATION OF CATHODE OVERALL CHARACTERISTICS

Estimates of conductivity of an active layer with combined grains allow us to embark on calculations of the overall characteristics of such cathodes. All necessary parameters taken in the below calculations are shown in the end of this paper. However, it is necessary to decide on the criterion of assessment of the cathode overall characteristics.

Table 1. Dependence of the reduced ionic conductivity of a combined grain on its reduced size

$N = L/d$	κ^{**}
2	0.298
4	0.147
6	0.117
8	0.111
10	0.108
12	0.106
14	0.106
16	0.105

Table 2. Dependence of the reduced ionic conductivity of combined grains involved in a percolation ionic cluster on the volume concentration of combined grains

g_s	κ*
0.35	0.0061
0.40	0.026
0.45	0.061
0.50	0.109
0.55	0.166
0.60	0.231
0.65	0.304

As was mentioned in the Introduction, our aim was not only to reach the highest values of overall current and power density but also to minimize the consumption of the catalyst (platinum). These two requirements are obviously contradictory, as clearly demonstrated in Fig. 4. The latter shows the dependence of the overall current of an air cathode with combined grains on the active layer thickness. The cathodic potential E_0 = 0.6 V, the reduced size of combined grains N = 2, the cathode temperature varied in such a way that in Fig. 4a, the curves *1–3* correspond to the following temperatures t: (*1*) 60, (*2*) 80, (*3*) 95°C.

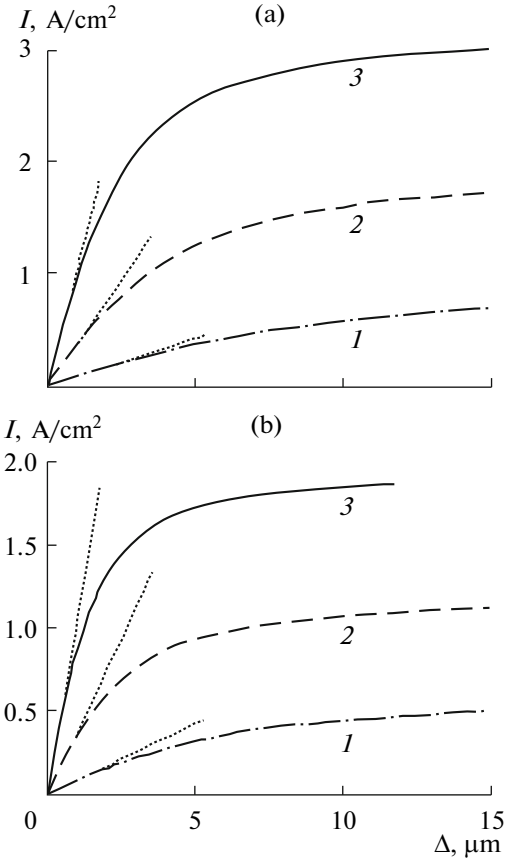

Fig. 4. Dependence of the overall current of an air cathode with combined grains on the active layer thickness. t, °C: (*1*) 60, (*2*) 80, (*3*) 95; (a) N = 2, (b) N = 8. Cathode potential E_0 = 0.6 V.

The specific content of the catalyst in the cathodic active layer with the thickness Δ can be assessed using the relationship

$$m = g_s(1 - \nu)\rho_s[g_w/(1 - g_w)]\,\Delta, \qquad (9)$$

where g_s is the volume concentration of carrier (carbon black) grains in the active layer, ν is the volume fraction of Nafion in a combined grain, ρ_s is the carbon material density, g_w is the mass content of platinum in the carrier. Assuming g_s = 0.65, ν = 0.5, ρ_s = 1.8 g/cm^3, g_w = 46 wt %, we find that 4.98×10^{-2} mg/cm^2 of platinum should be consumed per μm of the active layer. Thus, the platinum consumption, the same as the overall current, should increase with the increase in the active layer thickness.

However, the linear increase in the overall current is observed only for small active layer thicknesses (this becomes clear if we consider the dashed lines in Fig. 4). For large thicknesses, the overall current reaches its limiting value I_∞ attainable only at the limitless increase in the active layer thickness. Figure 4 clearly shows that it is unreasonable to try to obtain the overall current values that approach the limiting values, because this would be associated with the excessive consumption of the catalyst (platinum). The data in Table 3 quantitatively confirm the latter assumption.

Let us consider curve *2* in Fig. 4a. It is characterized by parameters N = 2, t = 80°C, the limiting current I_∞ = 1.856 A/cm^2. Let us plot the dependences of the overall current I and the specific consumption of platinum λ on the active layer thickness Δ or, which is virtually the same (Eq. (9)), on the specific content of the catalyst in the active layer m. With a decrease in the current (the first column in Table 3), the specific consumption of platinum also decreases (the last column in Table 3) tending to a certain lower limit.

Hence, calculating the overall characteristics of a cathode with combined grains, one should assume which part of the maximally possible overall current I_∞ he wants to obtain. Which of two quantities is more important, viz., the overall current I (and power density W) or the specific consumption of platinum λ? Where is the compromise between the trend to make a fuel cell more powerful and the desire to save platinum? The analysis of data in Table 3 shows that the desirable compromise could be, say, the criterion I/I_∞ = 0.7, if one compares the values of I and λ in the first, seventh, and the other lines of Table 3.

Yet another remark. Table 3 was built with an allowance made for the fact that the combined grain size is the minimum N = 2. And what happens if we increase N to N = 8 thus decreasing the conductivity of a combined grain? Table 4 gives the answer to this

question. A three-fold decrease in the combined grain conductivity leads to the 1.5-fold increase in the overall current and the decrease in the necessary content of platinum in the active layer by approximately the same factor. As a result, the data of the last columns in Table 3 and Table 4 turn out to be identical.

RESULTS OF CALCULATIONS OF OVERALL CHARACTERISTICS

The procedure of calculating the overall currents and other characteristics of active layers of cathodes with Nafion and platinum the Tafel plots of which demonstrate several segments with different slopes can be found in [21]. Figure 5 shows an example of calculation of overall characteristics for an air cathode with combined grains. It was assumed that the layer activity is the maximum ($N = 2$, $\kappa^{***} = 9.06 \times 10^{-3}\ \Omega^{-1}\ cm^{-1}$). As the criterion of estimates of overall characteristics, a condition $I = 0.7I_\infty$ was taken (the platinum content in the active layer m was chosen in such a way that the current generated at a given cathodic potential E_0 was 70% of the maximally possible value I_∞ at the same potential).

In Fig. 5a, for three temperatures ((*1*, *1*') 60, (*2*, *2*') 80, (*3*, *3*') 95°C), voltammetric curves (curves *1*–*3*) of an air cathode are plotted; in addition, under an assumption of the absence of Ohmic losses in the membrane, the power density of a hydrogen-air fuel cell is plotted as a function of the overall current (curves *1*'–*3*'). Figure 5b demonstrates the dependences of platinum consumption per kW of electricity on the cathode potential, plotted under the same assumption.

In a cathode with combined grains, attention is drawn to the very rapid increase in the overall current and power density. In cathodes with two types of grains (Fig. 1a), the overall voltammetric curves have two slopes, namely, 60 and 240 mV; hence, the power density reaches an extremum at approximately the cathodic potential $E_0 = 0.3$ V. At the same time, in cathodes with combined grains (Fig. 5a), the slopes of overall voltammetric curves are 60 mV and ca. 120 mV (because at the fulfillment of criterion $I = 0.7I_\infty$, the current in the active layer is generated by the kinetic mechanism). Thus, the power density of a cathode with combined grains reached an extremum later, at ca. $E_0 = 0.1$ V. For $E_0 = 0.4$ V, the overall current, the power density, and the specific consumption of platinum reached the following values. For $t - 60, 80, 95$°C, the current was 4.23, 8.92, and 14.85 A/cm^2, the power density was 1.69, 3.57, and 5.94 W/cm^2, the platinum consumption was 0.05, 0.01, and 0.004 g/kW. According to Table 5, with the decrease in the potential of a cathode with combined grains decreases, the specific consumption of platinum λ (the last column in Table 5) rapidly decreased.

Table 3. Dependence of the overall characteristics of an air cathode on the fraction of current generated in the cathode at potential $E_0 = 0.6$ V (model of combined grains, $N = 2$, $t = 80$°C, $I_\infty = 1.856$ A/cm^2)

I/I_∞	I, A/cm^2	Δ, μm	m, mg/cm^2	$\lambda = m/W$, g/kW
0.9	1.67	12.74	0.63	0.63
0.8	1.485	7.74	0.39	0.43
0.7	1.30	5.45	0.27	0.35
0.6	1.11	4.05	0.20	0.30
0.5	0.93	3.04	0.15	0.27
0.4	0.74	2.26	0.11	0.25
0.3	0.56	1.61	0.08	0.24
0.2	0.37	1.04	0.05	0.23
0.1	0.19	0.51	0.03	0.23

Table 4. Dependence of overall characteristics of an air cathode on the current fraction generated in the cathode at potential $E_0 = 0.6$ V (model of combined grains, $N = 8$, $t = 80$°C, $I_\infty = 1.132$ A/cm^2)

I/I_∞	I, A/cm^2	Δ, μm	m, mg/cm^2	$\lambda = m/W$, g/kW
0.9	1.02	7.77	0.39	0.63
0.8	0.91	4.72	0.24	0.43
0.7	0.79	3.325	0.17	0.35
0.6	0.68	2.47	0.12	0.30
0.5	0.57	1.86	0.09	0.27
0.4	0.45	1.38	0.07	0.25
0.3	0.34	0.98	0.05	0.24
0.2	0.23	0.63	0.03	0.23
0.1	0.11	0.31	0.02	0.23

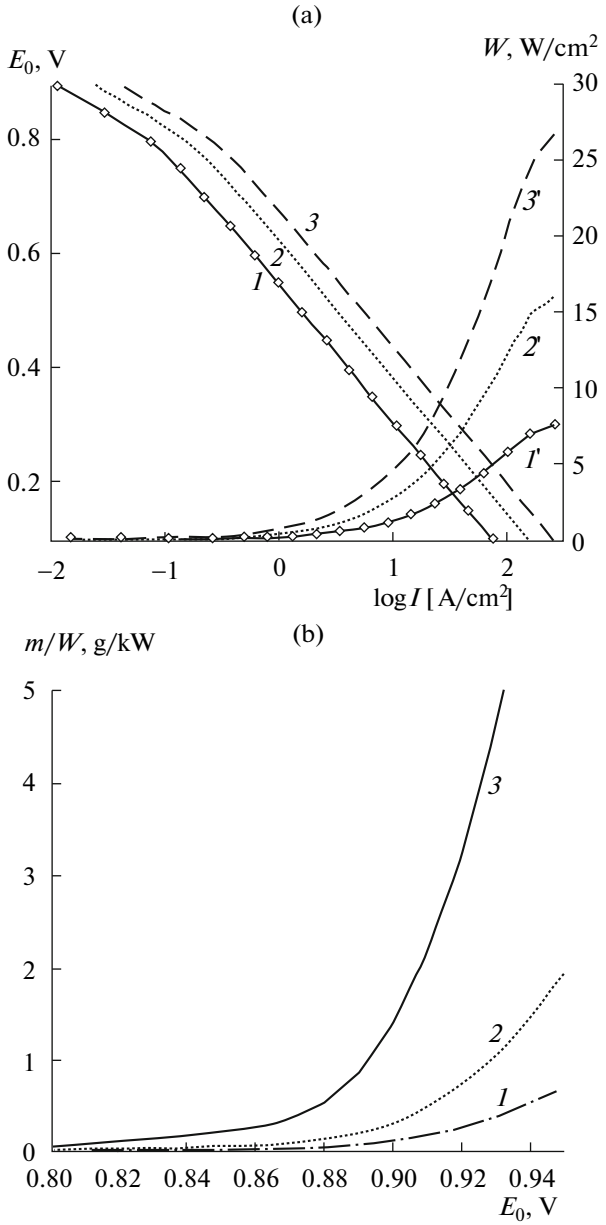

Fig. 5. (a, *1*–*3*) Voltammetric curves of an air cathode and (*1*'–*3*') dependences of the power density of a hydrogen-air fuel cell on the overall current; (b) dependences of the platinum consumption per kW of electric energy on the cathode potential. *t*, °C: (*1*, *1*') 60, (*2*, *2*') 80, (*3*, *3*') 95. $\delta = 0$, $N = 2$.

Also note that at $t = 80$°C and a cathodic potential $E_0 = 0.6$ V, we have the following values of overall characteristics: current $I = 1.30$ A/cm^2, power $W = 0.78$ W/cm^2, platinum consumption $\lambda = 0.35$ g/kW. It is expedient to compare these characteristics with the values shown in the Introduction, namely, $I = 1.17$ A/cm^2, $W = 0.7$ W/cm^2, parameter λ in the range of 0.85–1.1 g/kW. However, it should be noted that the first sequence of values pertains to the cathode, whereas the second sequence corresponds to the whole hydrogen-air fuel cell.

Comparing the overall characteristics of a cathode with combined grains with the characteristics of conventional cathodes, two factors should be taken into account. First, our calculations were carried out using a catalyst (TCC) with a low platinum content in carrier grains, $g_w = 46$ wt %, and relatively low specific surface $S^* = 86$ m^2/g Pt. Second, at lower cathodic potentials ($E_0 < 0.6$ V), the characteristics of a cathode with combined grains begin to dominate over those of a conventional active-layer cathode, as demonstrated by the data of Table 5 and Fig. 5.

Table 5. Dependence of overall characteristics of an air cathode on its potential (model of combined grains, $N = 2$)

E_0, V	$0.7\,I_\infty$, A/cm^2	Δ, μm	W, W/cm^2	m, mg/cm^2	$\lambda = m/W$, g/kW
$t = 60°C$, $i^* = 9.08 \times 10^{-3}$ A/cm^3					
0.7	0.23	28.82	0.162	1.44	8.885
0.65	0.38	18.38	0.246	0.92	3.72
0.6	0.62	11.50	0.370	0.57	1.55
0.55	1.00	7.14	0.549	0.36	0.65
0.5	1.62	4.425	0.808	0.22	0.27
$t = 80°C$, $i^* = 4.04 \times 10^{-2}$ A/cm^3					
0.7	0.49	14.00	0.341	0.68	2.00
0.65	0.80	8.71	0.519	0.43	0.84
0.6	1.30	5.45	0.780	0.27	0.35
0.55	2.11	3.39	1.158	0.17	0.15
0.5	3.41	2.10	1.704	0.10	0.06
$t = 95°C$, $i^* = 1.12 \times 10^{-1}$ A/cm^3					
0.7	0.81	8.205	0.568	0.41	0.72
0.65	1.33	5.23	0.865	0.26	0.30
0.6	2.16	3.275	1.298	0.16	0.13
0.55	3.51	2.03	1.929	0.10	0.05
0.5	5.68	1.26	2.838	0.06	0.02

Table 6. Dependence of overall characteristics of an oxygen cathode on the potential (model of combined grains, $N = 2$)

E_0, V	$0.7\,I_\infty$, A/cm^2	Δ, μm	W, W/cm^2	m, mg/cm^2	$\lambda = m/W$, g/kW
$t = 60°C$					
0.7	0.50	13.21	0.353	0.66	1.87
0.65	0.83	8.42	0.537	0.42	0.78
0.6	1.34	5.27	0.807	0.26	0.33
0.55	2.18	3.27	1.198	0.16	0.14
0.5	3.53	2.03	1.763	0.10	0.06
$t = 80°C$					
0.7	1.06	6.26	0.74	0.31	0.42
0.65	1.74	3.99	1.13	0.20	0.18
0.6	2.84	2.50	1.70	0.12	0.07
0.55	4.60	1.55	2.53	0.08	0.03
0.5	7.44	0.96	3.72	0.05	0.01
$t = 95°C$					
0.7	1.77	3.76	1.239	0.19	0.15
0.65	2.90	2.40	1.887	0.12	0.06
0.6	4.72	1.50	2.833	0.07	0.03
0.55	6.65	0.93	4.209	0.05	0.01
0.5	12.4	0.58	6.193	0.03	0.005

It is also expedient to show the results of calculations of overall characteristics for an oxygen cathode with combined grains. These characteristics are shown in Fig. 6 and Table 6. This cathode at $t = 80°C$ and potential $E_0 = 0.6$ V had the following parameters: current $I = 2.84$ A/cm^2, power $W = 1.70$ W/cm^2, platinum consumption $\lambda = 0.07$ g/kW. At $E_0 = 0.4$ V, the overall characteristics of an oxygen cathode with combined grains were as follows: for $t = 60, 80, 95°C$, the current was 9.23, 19.47, and 32.41 A/cm^2, the power was 3.69, 7.79, and

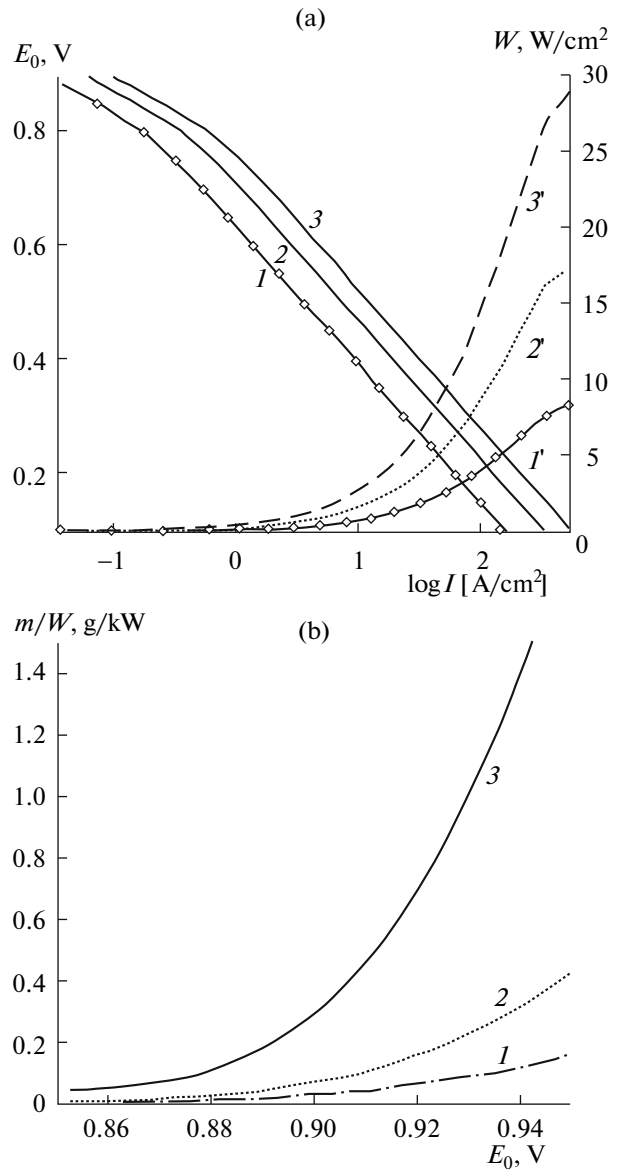

Fig. 6. (a) (*1*–*3*) Voltammetric curves of an oxygen cathode and (*1*'–*3*') dependences of the power density of a hydrogen-oxygen fuel cell on the overall current; (b) dependences of the platinum consumption per kW of electric energy on the cathode potential. t, °C: (*1*, *1*') 60, (*2*, *2*') 80, (*3*, *3*') 95. $\delta = 0$, $N = 2$.

12.96 W/cm^2, and the platinum consumption was 0.01, 0.0024, and 0.00085 g/kW, respectively.

CONCLUSION

It is proposed to fundamentally change the active layer structure in the cathode of a polymer electrolyte fuel cell. Its already traditional structure contains two types of grains, namely, agglomerates of Nafion molecules (proton carriers) and porous agglomerates of carbon black particles covered with fine platinum crystals (electron and gas carries, Knudsen diffusion). Now, we can restrict our consideration to a single type of grains, the so-called "combined grains" that represent nonporous agglomerates of carbon black and Nafion particles (which together provide the transfer of both protons and electrons in such a grain). On the other hand, oxygen or air can be delivered to the active layer with combined grains through gas pores.

Cathodes of this new type have several advantages over conventional cathodes. In a combined grain, the full contact is provided between platinum deposited on the surface of the carrier (carbon black) and Nafion, the proton-deliverer. As a result, the degree of catalyst utilization can be raised to 100%. Furthermore, in a cathode with combined grains, oxygen is delivered through coarse gas pores in which common molecular diffusion of the gas occurs. This is why the internal diffusion limitations in the active layer with combined grains become negligibly small. And, finally, in the active layer of a cathode with combined grains, the danger that the gas pores get flooded with the evolved moisture is virtually nonexistent.

Yet another advantage of the oxygen and air cathodes with combined grains, which is the main result of this study, is that as compared with conventional cathodes, such a cathode exhibits not only the enhanced power density but also the lower index of platinum consumption, i.e., platinum mass per kW of electric energy produced in the membrane-electrode block (MEB).

It is important to add the following. The idea of possibility of forming combined grains and the merits of its use in the active layer structure in cathodes with polymer electrolyte (Nafion) emerged after the completion of our previous paper [22] (see also [23]). There, a detailed computer simulation of the penetration of fine Nafion fractions into the catalyst carrier grains was carried out. The set of factors was revealed that involved the grain size, the size of carbon black particles that constitute this grain, and the size of fragments of polymer electrolyte molecules, all of which affected the formation of a proton-conducting fractal Nafion film on the surface of pores in the carrier grains. It was also proved that it is the filling of carrier grains with Nafion that explains the seemingly paradoxical fact, viz., the experimentally observed high degree of platinum utilization in cathodes with polymer electrolytes. Thus, the concept of combined grains now has a well-developed theoretical substantiation and contains direct recommendations that allow one to increase the filling of carrier grains with the polymer electrolyte.

LIST OF DESIGNATION OF PARAMETERS CHARACTERIZING A FUEL CELL WITH NAFION AND PLATINUM AND THEIR VALUES TAKEN IN CALCULATIONS

$t = 60$, 80, and 95°C are fuel cell temperatures

$p^* = 101$ kPa is the pressure in the gas chamber

Δ is the active layer thickness

m, mg/cm^2 is the cathode loading with platinum

$E_{st} = 1.05$ V is the steady-state potential of cathode

$E^* = 0.825$ V is the breakpoint potential in the polarization curve of oxygen reduction on platinum

E_0 is the cathode potential

I_∞, A/cm^2 is the limiting overall current of the cathode

$\lambda = m/W$, g/kW is the specific consumption of platinum in the cathode active layer

$b_1 = 2.6 \times 10^{-2}$ V is the Tafel plot slope in the high potential range

$b_2 = 5.2 \times 10^{-2}$ V is the Tafel plot slope in the low potential range

$n = 4$ is the number of electrons involved in the electrochemical reaction

$F = 9.6 \times 10^4$ C/mol is the Faraday number

$i_0 = 10^{-8}$ A/cm^2 is the exchange current in the high potential range at $t = 50$°C

$g_w = 46$ wt % is the platinum content in carrier grains (TCC catalyst)

$\eta = 100\%$ is the degree of catalyst (platinum) utilization in a combined grain

$S^* = 86$ m^2/g Pt is the specific surface of catalyst (platinum) per its mass unit (TCC catalyst)

$\nu = 0.5$ is the volume fraction of Nafion in a combined grain

$\rho_p = 21.5$ g/cm^3 is the catalyst (platinum) density

$\rho_s = 1.8$ g/cm^3 is the carrier (carbon black) density

i^*, A/cm^3: 9.08×10^{-3}, 4.04×10^{-2}, 1.12×10^{-1} are the characteristic volume current densities at $t = 60$, 80, and 95°C

$L = 60$ and 240 nm is the length of carrier grain edges

$d = 30$ nm is the pore size in carrier grains

$N = L/d = 2$ and 8 is the reduced size of a combined grain

$g_s = 0.65$ is the volume concentration of combined grains

$g_0 = 0.35$ is the volume concentration of pores in the active layer with combined grains

$\kappa = 0.1$ Ω^{-1} cm^{-1} is the specific conductivity of Nafion with the optimum moisture content

$\kappa^{**} = 0.298$ and 0.111 is the reduced conductivity of carrier grains

$\kappa^* = 0.304$ is the reduced specific ionic conductivity of combined grains in a percolation ionic cluster

$\kappa^{***} = 9.06 \times 10^{-3}$ and 3.37×10^{-3} Ω^{-1} cm^{-1} is the specific ionic conductivity of Nafion in an active layer with combined grains

$\delta = 0$ is the Nafion membrane thickness in a fuel cell (in the absence of Ohmic limitations in the membrane).

REFERENCES

1. Wheeler, D.J., Yi, J.S., Fredley, R., Yang, D., Patterson, Jr. T., and VanDine, L., *J. New Mater. Electrochem. Syst.*, 2001, vol. 4, p. 233.
2. Gasteiger, H.A., Kocha, S.S., Sompalli, B., and Wagner, F.T., *Appl. Catal. B*, 2005, vol. 56, p. 9.
3. Costamagna, P. and Srinivasan, S., *J. Power Sources*, 2001, vol. 102, p. 242.
4. Springer, T.E. and Gottesfeld, S., in *Modeling of Batteries and Fuel Cells*, White, R.E., Verbrugge, M.W., and Stockel, J.F., Eds., PV 91-10, Electrochem. Soc. Proc. Series, New York: Pennington, 1991, p. 197.
5. Gottesfeld, S. and Zawodzinski, T.A., in *Advances in Electrochemical Science and Engineering*, Tobias, C., Ed., New York: Wiley, 1997, vol. 5.
6. Perry, M.I., Newman, J., and Cairns, E.J., *J. Electrochem. Soc.*, 1998, vol. 145, p. 5.
7. Eikerling, M. and Kornyshev, A.A., *J. Electroanal. Chem.*, 1998, vol. 453, p. 89.
8. Wang, C.Y., *Chem. Rev.*, 2004, vol. 104, p. 4727.
9. Weber, A.Z. and Newman, J., *Chem. Rev.*, 2004, vol. 104, p. 4679.
10. Mukherjee, P. and Wang, C.-Y., *J. Electrochem. Soc.*, 2006, vol. 153, no. 5, p. A840.
11. Chirkov, Yu.G. and Rostokin, V.I., *Elektrokhimiya*, 2004, vol. 40, p. 1036 [*Russ. J. Electrochem.* (Engl. Transl.), vol. 40, p.].
12. Chirkov, Yu.G. and Rostokin, V.I., *Elektrokhimiya*, 2008, vol. 44, p. 1321 [*Russ. J. Electrochem.* (Engl. Transl.), vol. 44, p.].
13. Chirkov, Yu.G. and Rostokin, V.I., *Elektrokhimiya*, 2006, vol. 42, p. 799 [*Russ. J. Electrochem.* (Engl. Transl.), vol. 42, p.].
14. Efros, A.L., *Fizika i Geometriya Besporyadka* (Physics and Geometry of Disorder), Moscow: Nauka, 1982.
15. *Percolation Structures and Processes*, Deutscher, G., Zallen, R., and Adler, J., Eds., Bristol: Hilger, 1983.
16. Tarasevich, Yu.Yu., *Perkolyatsiya: teoriya, prilozheniya, algoritmy* (Percolation: Theory, Applications, Algorithms), Moscow: Editorial URSS, 2002.
17. Kirkpatrick, S., *Rev. Mod. Phys.*, 1973, vol. 45, p. 574.
18. Stauffer, D., *Phys. Reports*, 1979, vol. 54, p. 1.
19. Chirkov, Yu.G., *Elektrokhimiya*, 1999, vol. 35, p. 1449 [*Russ. J. Electrochem.* (Engl. Transl.), vol. 35, p.].
20. Uchida, M., Aoyama, Y., Eda, N., and Ohta, A., *J. Electrochem. Soc.*, 1995, vol. 142, p. 4143.
21. Chirkov, Yu.G. and Rostokin, V.I., *Elektrokhimiya*, 2006, vol. 42, p. 806 [*Russ. J. Electrochem.* (Engl. Transl.), vol. 42, p.].
22. Chirkov, Yu.G. and Rostokin, V.I., *Elektrokhimiya,* 2009, vol. 45, p. 1376 [*Russ. J. Electrochem.* (Engl. Transl.), vol. 45, p.].
23. Chirkov, Yu.G. and Rostokin, V.I., Abstracts of Papers *II Vseros. konf. "Mnogomasshtabnoe modelirovanie protsessov i struktur v nanotekhnologiyakh"* (II All-Russian Conference "Multiscale Modeling of Processes and Structures in Nanotechnologies), Moscow, 2009, p. 458.